

# Optical Engineering

[SPIDigitalLibrary.org/oe](http://SPIDigitalLibrary.org/oe)

## **Modal analysis of a large-mode area photonic crystal fiber amplifier using spectral-resolved imaging**

Marko Laurila  
Thomas T. Alkeskjold  
Jesper Lægsgaard  
Jes Broeng

# Modal analysis of a large-mode area photonic crystal fiber amplifier using spectral-resolved imaging

## Marko Laurila

Technical University of Denmark  
Department of Photonics Engineering  
DTU Fotonik  
Kgs. Lyngby, 2800 Denmark  
E-mail: malau@fotonik.dtu.dk

## Thomas T. Alkeskjold

NKT Photonics  
Blokken 84  
Birkerød, 3460 Denmark

## Jesper Lægsgaard

Technical University of Denmark  
Department of Photonics Engineering  
DTU Fotonik  
Kgs. Lyngby, 2800 Denmark

## Jes Broeng

NKT Photonics  
Blokken 84  
Birkerød, 3460 Denmark

## 1 Introduction

Ytterbium-doped fibers with large-mode area (LMA) have attracted many new applications both in the scientific and industrial worlds. The demand for higher output powers has pushed fibers toward having a larger and larger effective area ( $A_{\text{eff}}$ ) to mitigate nonlinearities. With increasing  $A_{\text{eff}}$ , the fibers easily support an increasing number of higher-order modes (HOMs), which limits the pointing stability of the output beam. However, photonic-crystal fibers (PCFs) have unique properties compared to standard step-index LMA fibers and can be engineered to suppress or not guide HOMs and thus increase pointing stability.<sup>1,2</sup>

The criterion for single-mode operation is, according to the ANSI/TIA-455-80-C standard, that the HOMs should be suppressed more than 19.3 dB by a 28-cm coil, which is typically measured by the bent reference cutoff method.<sup>3</sup> We refer to this standard because it describes how to measure cutoff wavelength of uncabled single-mode fibers by transmitted power and because it is generally accepted in the field of optical fibers as the common method of quantifying whether a fiber is single mode or not. However, this method has proven to be difficult for LMA PCFs due to the low numerical aperture (NA) of the core and the strongly wavelength-dependent NA, which, for example, gives rise to a short-wavelength bend-loss edge in PCFs.<sup>4</sup>

Currently, the  $M^2$  parameter is commonly used to define the quality of the laser beam and an  $M^2$  number close to 1 is typically a measure of single-mode operation. However, it has been shown that a low  $M^2$  number is not a guarantee for

**Abstract.** We perform modal characterization on an ytterbium-doped large mode area photonic-crystal-fiber (PCF) amplifier using spatial and spectral ( $S^2$ ) resolved imaging and compare results to conventional cutoff methods. We apply numerical simulations and step-index fiber experiments to calibrate our mathematical and experimental routines of our  $S^2$  imaging system. We systematically analyze higher-order-mode (HOM) content of a polarizing 40- $\mu\text{m}$  core double-clad PCF amplifier with various launching and coiling configurations. We demonstrate a HOM suppression of more than -24 dB with variance of 2.3 dB. © 2011 Society of Photo-Optical Instrumentation Engineers (SPIE). [DOI: 10.1117/1.3609816]

Subject terms: spectral resolved imaging; photonic crystal fibers.

Paper 110408SSPR received Apr. 22, 2011; revised manuscript received Jun. 1, 2011; accepted for publication Jun. 20, 2011; published online Oct. 5, 2011.

single-mode operation.<sup>5</sup> Recently, a new method described by Nicholson *et al.*<sup>6</sup> uses spatial and spectral ( $S^2$ ) interferometry to spatially resolve propagating modes and their relative intensities. This method can be directly applied for measuring the HOM suppression of optical fibers. The suppression is defined as the differential loss between the HOM and the fundamental mode in a doped but unpumped fiber.

In this paper, we demonstrate the use of an  $S^2$  imaging technique on a flexible LMA PCF. We evaluate the single-mode performance of the PCF by investigating the HOM content under different operating conditions, such as offset launch and fiber coil diameter.

Few experimental  $S^2$  imaging systems have been demonstrated previously.<sup>6-13</sup> However, none relate the  $S^2$  imaging results to a conventional cutoff-wavelength method.<sup>3</sup> We construct an  $S^2$  imaging system and verify the operation of our mathematical routines using numerical simulations. In addition, we perform the  $S^2$  imaging on a step-index fiber with known HOM suppression in order to verify the operation of our experimental system. In our experiments, we analyze the HOM content of an ytterbium-doped flexible photonic crystal fiber under different launching conditions and coiling diameters, in a passive configuration, without introducing any pump light. We limit our experiments only to the passive configuration, avoiding any gain-related phenomena corrupting the results, such as gain competition of different modes.

## 2 Spectral-Resolved Imaging

Two or more modes propagating in an optical fiber form a spatial and spectral interference pattern if the modes have different group velocities. The  $S^2$  imaging method analyzes this

interference pattern and can detect small quantities of HOMs interfering with the fundamental mode. No prior knowledge of the fiber properties are required to fully quantify the modal shape of the different modes and their relative intensities and phases.<sup>6-8</sup>

Following the analysis on Ref. 6, we can analyze the amount of different modes in the core of the fiber and calculate the HOM suppression. For further insight into the measuring modal content of LMA fibers, readers are referred to Ref. 6.

### 3 Experiments

#### 3.1 Experimental Measurement System

The experimental setup is shown in Fig. 1. An ytterbium-doped amplified spontaneous emission (ASE) source, consisting of three core-pumped stages, gives a stable, single-mode, and broadband ASE spectrum between 1040 and 1070 nm. This is used to seed a test fiber and generate interference patterns when the  $S^2$  imaging measurement is performed. The ASE source is coupled into the test fiber using two mirrors and lenses for studying the modes of the fiber, by offsetting the input beam and deliberately exciting HOMs. The test fibers are always polarization maintaining, and a polarizer is used to launch the light along the slow polarization axis of the test fiber. The orientation of the slow axis is horizontal and along the  $x$ -axis when the stress rods are in the horizontal plane. The test fiber is coiled in a specific coil diameter. The near field of the test fiber is imaged onto a single-mode fiber (HI1060) probe with a set of two lenses, with a magnification of roughly 13 times. The fiber probe is mounted on motorized stages to ensure accurate and fast movements in the cross section of the output beam and is connected to a standard optical spectrum analyzer (OSA). The scanning time of one full measurement, consisting of a  $31 \times 31$  matrix, is limited due to the speed of the OSA. A polarizer at the output side is used to align the polarization of the modes along the same polarization axis.

We use commercial mathematical software Matlab for the mathematical routines and for calculating the HOM suppression measured with the  $S^2$  imaging setup. All the measured spectra are converted to frequency, then interpolated and re-sampled to get equal sampling spacing. The spectra are then remodulated by a Hamming sampling window in order to reduce the sampling-related broadening, which increase the effective resolution of the fast Fourier transforms (FFTs).

#### 3.2 Calibration of the $S^2$ Imaging System

We numerically calibrated our mathematical routines by constructing an  $S^2$  emulator using simulated modes. We simulated the modal fields and propagation constants using a

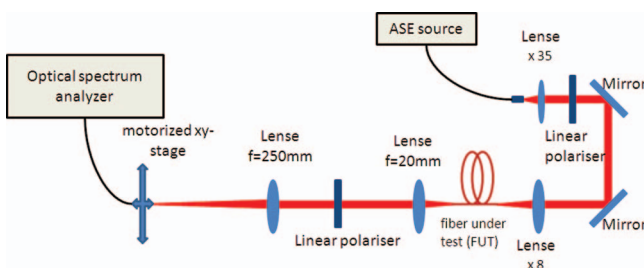


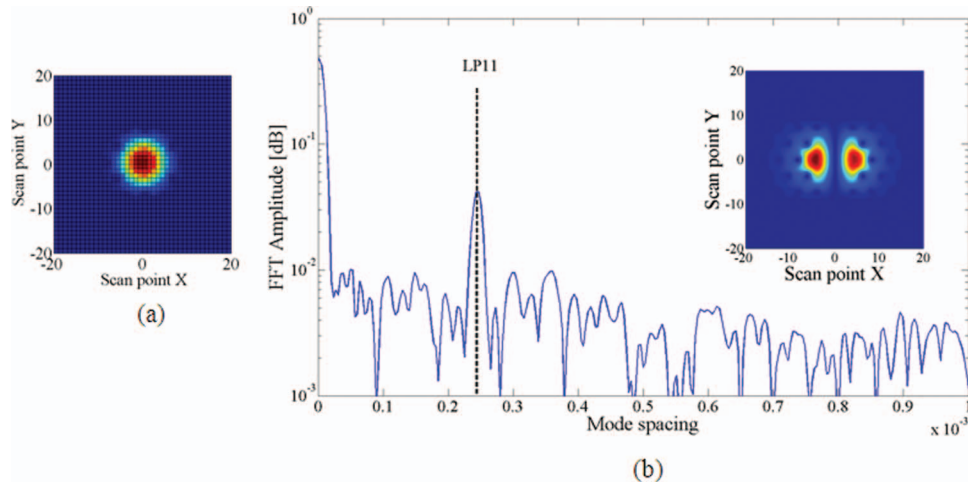
Fig. 1 Experimental  $S^2$  imaging setup.

commercial finite element solver (JCMWave GmbH, Berlin, Germany), which includes the stress distribution from the stress rods. We propagated the modes and calculated the spectral interference pattern in each of the spatial measurement points. Figure 2(a) shows the simulated intensity profile after propagating a LP01 and LP11 mode in the photonic crystal fiber when the HOM/LP11 content is 100 times weaker than the fundamental mode. Fourier transform of the optical interference spectrum in one spatial point of the simulated intensity profile is shown in Fig. 2(b). The Fourier spectrum is shown as a function of mode spacing, which is defined by the effective index difference between the interfering modes. The mode spacing is calculated using the relation  $\Delta n = \lambda^2 / (\Delta \lambda \cdot L)$ , where  $\Delta n$  is the mode spacing,  $\lambda$  is the wavelength,  $L$  is the fiber length, and  $1/\Delta \lambda$  is the frequency obtained with the FFT. The Fourier spectrum shows two spectral components at 0 and  $0.23 \times 10^{-3}$  corresponding to the fundamental mode and the LP11 mode suppressed by  $-20$  dB, respectively. The inset of Fig. 2(b) shows the reconstructed LP11 mode profile. The reconstructed LP11 mode profile is postprocessed by increasing the sampling rate by simply interpolating the gray scale map index value across the image. This is done after the HOM suppression is calculated, only to give a better visualization for the reader, and therefore not effecting the HOM suppression calculations.

In addition, we experimentally validated our  $S^2$  imaging system by using a 1-m-length polarization maintaining step-index LMA fiber with 0.06 NA and  $15\text{-}\mu\text{m}$  mode field diameter, illustrated in the inset of Fig. 3. The principle is to use a fiber with known HOM suppression, which can be measured with a standard spectral transmission measurement, and relate these results on to  $S^2$  imaging measurement. We characterized the modal properties of the fiber in two different bent configurations and measured the relative power difference. We identified a slight bent configuration, where the HOM content was suppressed by  $\sim 20$  dB at 1045 nm. This wavelength was identified by measuring the transmission spectrum for the fiber when it was straight and also slightly bent with a minimum radius curvature of 65 cm.

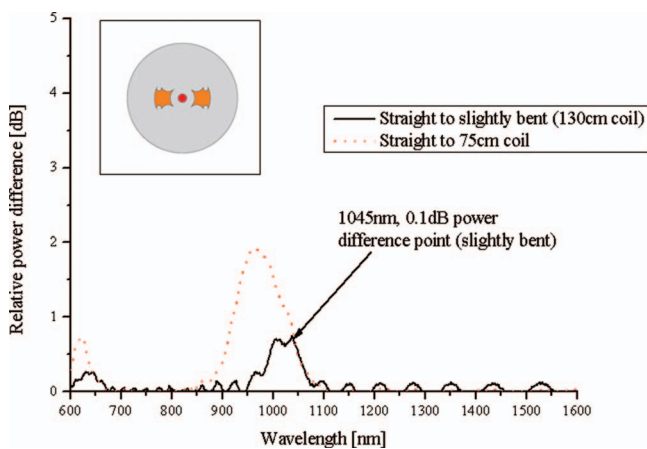
Figure 3 shows the relative intensity difference between the two measured spectra and a 0.1-dB difference in transmission at the 1045-nm wavelength for a slightly bent configuration, 130-cm coiling diameter (solid line). When the fiber was bent more, 75 cm, (dotted line), the 0.1-dB transmission difference moves to  $\sim 950$  nm. At that wavelength, the HOMs carry 2.27% of the power and the relative power difference (suppression) between the HOMs and the fundamental mode is then  $-16.4$  dB. However, when the measurement was performed, the light was coupled into the fiber by overfilling the NA of the core, and thus all the supported modes were excited. Therefore, two HOMs and only one fundamental mode were excited. This means that the HOM suppression is, assuming the power is split equally between the two HOMs, 3 dB larger (i.e.,  $-19.4$  dB) and the HOM suppression should therefore be expected to be around  $-20$  dB at the 1045-nm wavelength.

Figure 4 shows the simulated LP01 and LP11 mode profiles supported by the fiber. These modes can be selectively excited by offsetting the input beam waist either along the  $y$ - or  $x$ -axis direction, exciting either LP11 mode oriented along the  $y$ - or  $x$ -axis, together with the fundamental mode. We used the same finite element solver as in the earlier simulations.



**Fig. 2** (a) Simulated intensity profile of the fundamental mode and the 100 times weaker higher order mode after traveling through a standard PCF of 40- $\mu\text{m}$  core diameter. (b) Example Fourier transform, shown as a function of mode spacing, which is defined by the effective index difference between the interfering modes, and reconstructed intensity profile of the  $-20\text{-dB}$  suppressed LP11 mode.

Several  $S^2$  imaging measurements were performed on the same fiber using three different coupling conditions, trying to excite HOMs in a simply and repeatable way: (i) Fundamental mode coupling, input signal was coupled into the core optimizing the overlap between the input beam and the fundamental mode of the fiber; (ii)  $y$ -axis LP11 mode coupling, offsetting the input beam orthogonal to the stress rod elements; (iii)  $x$ -axis LP11 mode coupling, offsetting the input beam toward the stress rod elements. These coupling configurations attempt to deliberately excite significant content of the HOMs and proves some degree of repeatability. The  $y$ - or  $x$ -axis LP11 mode coupling condition was found by translating the input beam off center along the  $y$ - or  $x$ -axis, until a  $-3\text{-dB}$  power drop was measured for the fundamental mode. This power drop was measured by placing the pickup fiber in the middle of the output beam, where the fundamental mode has the highest intensity and the LP11 mode has close to zero intensity. Therefore,  $\sim 50\%$  of the power was coupled to the fundamental and the remaining  $\sim 50\%$  was coupled



**Fig. 3** Transmission measurement of a polarization maintaining step-index LMA fiber with a 0.06 NA and 15  $\mu\text{m}$  mode field diameter, showing the wavelength where the HOM content is suppressed by  $-20\text{ dB}$ . The fiber design is illustrated in the inset.

mainly to the LP11 modes, but also to nonguided cladding modes.

The fiber was aligned with the stress rod elements in the horizontal plane and linearly polarized broadband light, between 1040 and 1070 nm, was coupled to the fiber in the slow polarization axis. The measured intensity profile is shown in Fig. 5(a), and an example of three Fourier transforms at different scan points of the measured beam are shown in Fig. 5(b), one calculated in the center of the beam and two at the full width half maxima of the beam. The Fourier transforms show clear presence of the LP11 mode, which was identified by calculating the theoretical mode spacing between the fundamental mode and the LP11 mode. Other spectral components, after the LP11 mode peak, correspond coupling between the fundamental mode and HOMs throughout the length of the fiber and, therefore, they appear as multiple peaks rather than a one peak. This is called distributed scattering and is described in detail in Ref. 7. The reconstructed LP11 mode is shown in the inset of Fig. 5(b), and the measured HOM suppression is  $-24.1\text{ dB}$

Figure 6 shows a histogram of the measured HOM suppression while varying the integration window width of the Fourier transforms, when performing HOM suppression calculations, and using different launching conditions. The average HOM suppression is  $-22.5\text{ dB} \pm 3\text{ dB}$ , which agrees reasonably well with the expected value ( $-20\text{ dB}$ ) obtained with the bent transmission reference method.

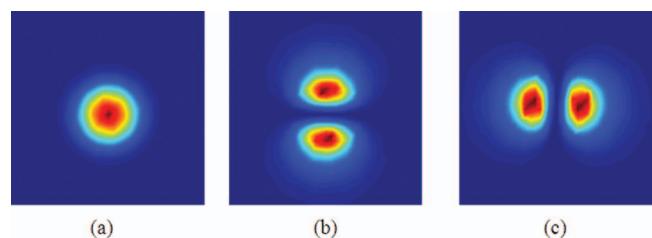


**Fig. 4** Simulated intensity profiles: (a) Fundamental mode (LP01), (b) LP11 mode oriented along the  $y$ -axis, and (c) LP11 mode oriented along the  $x$ -axis.

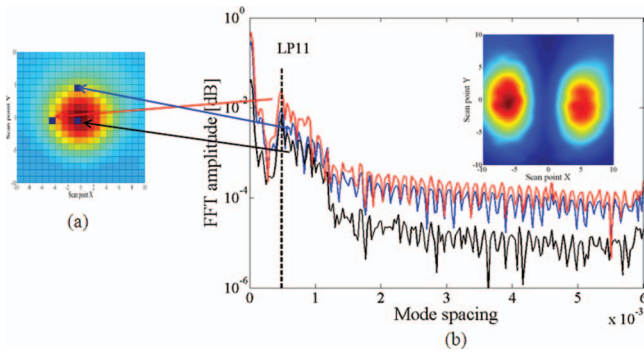


**Fig. 5** Example of the  $S^2$  imaging measurement on a 1-m length polarization maintaining LMA step-index fiber with 0.06NA and 15- $\mu\text{m}$  mode field diameter: (a) Typical intensity profile and (b) example Fourier transforms at three different scan points, shown with dark dots on (a) and reconstructed intensity image of the LP11 mode, HOM suppression  $-24.1$  dB.

### 3.3 $S^2$ Imaging of Ytterbium-Doped PCF

The  $S^2$  imaging was performed on a 2.2-m-length polarizing ytterbium-doped PCF (DC-200/40-PZ-Yb-03, NKT photonics, Birkerød, Denmark). The fundamental core mode had a 29- $\mu\text{m}$  mode field diameter, having an NA of 0.03 at 1064 nm. The multimode pump cladding was 200  $\mu\text{m}$ , having an NA of 0.6, as shown in Fig. 7.

PCF LMA fibers are sensitive to bending, especially if the bending plane is not aligned with the stress rod elements.<sup>12</sup> The flat sides of the outer fiber structure, shown in Fig. 7, will automatically orientate the fiber along the stress rod axis, thus avoiding twist, while coiling the fiber. This is referred to as “coil control.” In addition, because the fiber is always oriented along the stress rod elements, the modal stability is increased and the unwanted bend loss for the fundamental mode is reduced.

Low HOM content is difficult to analyze if the signal-to-noise level is not high enough (the term noise here is understood as light coupled into the cladding). Therefore, we infiltrated the air cladding of the test fiber with a cladding

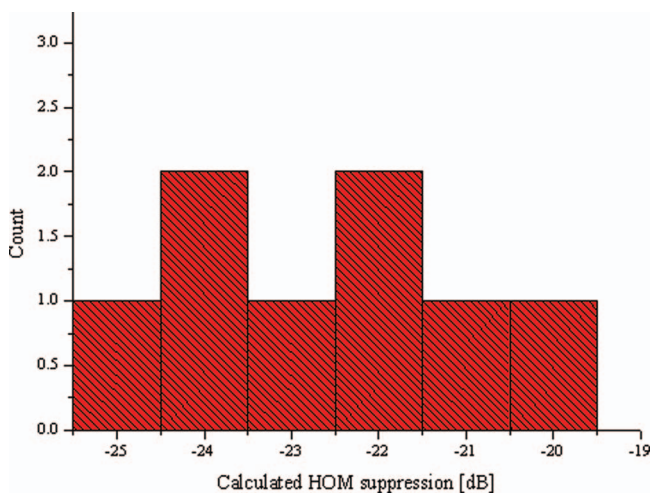


**Fig. 6** Histogram of the measured HOM suppressions obtained with the  $S^2$  imaging, while offsetting the input beam and varying the width of the Fourier integration window when calculating the HOM suppression. The average HOM suppression is  $-22.5 \pm 3$  dB.

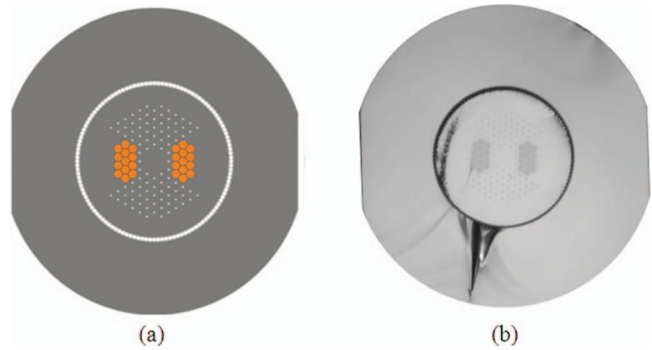


**Fig. 7** Fiber structure of DC-200/40-PZ-Yb-03: (a) Schematic of the fiber design illustrating the flat sides on each side of the stress rod elements and (b) optical micrograph picture of the fiber.

mode stripper (Glycerol) for 25 cm at the output end of the fiber and achieved an increase in signal-to-noise level from 25 to 37 dB. Linearly polarized light, between 1040 and 1070 nm, was coupled into the slow polarization axis of the test fiber with optimized mode matching between the coupled light and the fundamental mode of the fiber. The test fiber was coiled to a 28-cm coiling diameter, according to the TIA-455-80C standard,<sup>3</sup> and three different coupling conditions were used, as described earlier.

The measurement was repeated five times for the same fiber, and each time the fiber was recoiled and both ends were recleaved. Additional measurements were performed with a 40-cm coiling diameter. Typical intensity profile obtained with the  $S^2$  imaging is shown in Fig. 8(a). An example of Fourier transforms in three different points, as described before, of the measured beam is shown in Fig. 8(b), and the reconstructed LP11 mode is shown in the inset of Fig. 8(b). Only the LP11 mode has clearly observable peaks in the Fourier spectrum, and the mode spacing matches the calculated value. Other HOMs were not found, even when offsetting the input beam. However, as in the earlier experiments with the step-index fiber, distributed scattering throughout the fiber length gives rise to the other spectral components observed after the main peak.

Table 1 shows the calculated HOM suppression of the five  $S^2$  imaging measurements performed on the fiber. Using the fundamental mode coupling condition, the LP11 mode

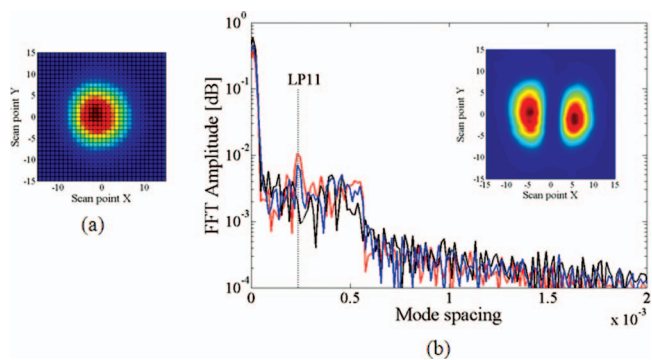


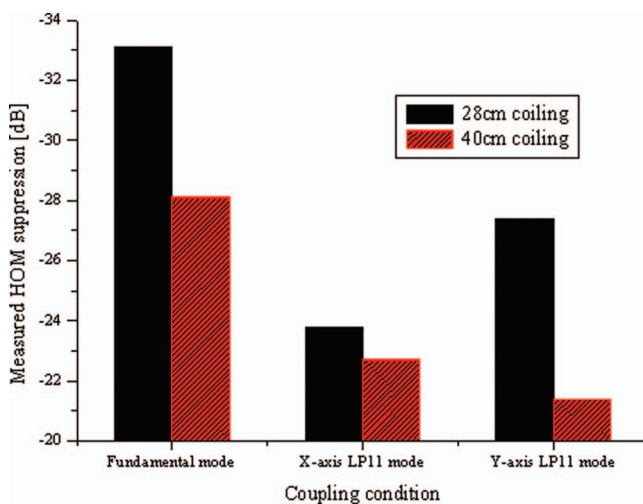
**Fig. 8** Example of the  $S^2$  imaging on a 2.2-m DC-200/40-PZ-Yb-03 having 29- $\mu\text{m}$  mode field diameter and NA of 0.03: (a) Example intensity profile and (b) example Fourier transforms at three different points at the beam, selected as in Fig. 5, and the reconstructed intensity image of LP11 mode, HOM suppression  $-24.7$  dB.

**Table 1** Summary of five  $S^2$  imaging measurements on a 2.2-m-length DC-200/40-PZ-Yb-03 coiled to a 28-cm diameter using three different coupling conditions.

Measurement	HOM suppression (dB)		
	Fundamental mode coupling	x-axis LP11 mode coupling	y-axis LP11 mode coupling
1	-33.1	-23.8	-28.6
2	-33.7	-27.7	-30.4
3	-31.5	-24.5	-23.2
4	-33.4	-25.9	-26.2
5	-31.6	-21.7	-24.5
<b>Average (dB)</b>	<b>-32.7</b>	<b>-24.7</b>	<b>-26.6</b>
<b>STDV (dB)</b>	<b>1.0</b>	<b>2.3</b>	<b>2.9</b>

is relatively weak with an average suppression of  $-32.7$  dB. As also studied in Ref. 10, when offsetting the input beam, one lobe of the LP11 mode overlaps with the input beam and is excited. Depending on the offsetting direction, either a LP11 mode along the  $y$ - or  $x$ -axis is excited. The LP11 mode oriented along the  $x$ -axis, shown in Fig. 4(c), has the stress rod element barrier, while the fiber is coiled, and therefore is less sensitive on bend loss than the LP11 mode oriented along the  $y$ -axis. For this reason, in the  $x$ -axis LP11 mode coupling, the HOM suppression is smaller ( $-24.7$  dB) than with the  $y$ -axis LP11 mode coupling ( $-26.6$  dB).

One important factor when performing the  $S^2$  imaging measurement is the coupling repeatability between various measurements. Even a slight error, for example, on the coupling angle will change the overlap between the input beam and the different modes in the fiber. Therefore, we chose to use the previously described three coupling conditions and they seemed to give fairly repeatable results, a standard deviation of  $<3.0$  dB.

**Fig. 9** Measured HOM suppression of a 2.2-m length DC-200/40-PZ-Yb-03, using two bending diameters.

In our last experiment, we performed the  $S^2$  imaging measurement having the bent diameter increased from 28 to 40 cm. The test fiber was the same as in our earlier measurements, and as before, we varied the coupling conditions.

Figure 9 illustrates the measured HOM suppressions for two bending diameters and three launching conditions. The stress rod element barrier effect is efficient for the LP11 mode oriented along the  $x$ -axis, and therefore, the measured HOM suppression are lower for the both bending diameters. However, the LP11 mode oriented along the  $y$ -axis is more susceptible to bend loss, and therefore, less HOM suppression is measured at 40-cm bend diameter.

Finally, in this work, we have focused on double-clad fibers, where all modes (including core and cladding modes) are confined within a low-index outer cladding. Although it is beyond the scope of the present work to analyze the influence of the outer cladding on the modal content, readers are refer to important work on the modal properties of core pumped LMA fibers in Ref. 13.

## 4 Conclusions

The  $S^2$  imaging is a relatively new measurement technique offering both spectral and spatially resolved data only in one measurement. Being an interferometric method, the  $S^2$  imaging is extremely sensitive and can characterize multiple HOMs simultaneously from LMA fibers, where conventional  $M^2$  or cutoff measurements fail. One limiting factor of the  $S^2$  imaging is the relatively long measurement time  $\sim 40$  min and stable launching conditions into the fiber, and nonmechanical perturbations on the fiber are required.

We demonstrated the  $S^2$  imaging on a flexible ytterbium-doped LMA photonic crystal fiber amplifier having a  $29\text{-}\mu\text{m}$  mode field diameter. The content of the strongest HOM, in this case the LP11 mode, was relatively low compared to the fundamental mode. Even when offsetting the input beam on purpose, exciting HOMs in a repeatable way, the measured HOM content at the output of the fiber did not significantly increase. The relative power difference, the HOM suppression, between the HOM and the fundamental mode was more than  $-24$  dB, when the fiber was coiled to 28 cm diam.

### Acknowledgments

The authors thank Siddharth Ramachandran and Kim P. Hansen for helpful discussions. The authors also acknowledge the support of the EU funded FP7 ALPINE Project No. 229231 and The Danish Council for Independent Research and Technology and Production Sciences.

### References

1. T. A. Birks, J. C. Knight, and P. S. J. Russell, "Endlessly single-mode photonic crystal fiber," *Opt. Lett.* **22**, 961–963 (1997).
2. K. P. Hansen, J. Broeng, A. Paterson, P. M. W. S. Martin, D. Nielsen, C. Jakobsen, and H. R. Simonsen, "High-power photonic crystal fibers," *Proc. SPIE*, **6102**, 61020B-1-11 (2006).
3. TIA Standards, FOTP-80 IEC-60793-1-44 Optical Fibres—Part 1-44: "Measurement methods and test procedures—cut-off wavelength," (2003).
4. T. Sørensen, J. Broeng, A. Bjarklev, E. Knudsen, and S. B. Libori, "Macro-bending loss properties of photonic crystal fibre," *Electron. Lett.* **37**, 287–289 (2001).
5. S. Wielandy, "Implications of higher-order mode content in large-mode-area fibers with good beam quality," *Opt. Express* **15**, 15402–15409 (2007).
6. J. W. Nicholson, A. D. Yablon, S. Ramachandran, and S. Ghalmi, "Spatial and spectrally resolved imaging of modal content in large-mode-area fibers," *Opt. Express* **16**, 7233–7243 (2008).
7. J. W. Nicholson, A. D. Yablon, J. M. Fini, and M. D. Mermelstein, "Measuring the modal content of large-mode-area fibers," *IEEE J. Sel. Top. Quantum Electron.* **15**, 61–70 (2009).
8. J. W. Nicholson, J. Jasapara, A. DeSantolo, E. Monberg, and F. Dimarcello, "Characterizing the modes of a core-pumped, large-mode area Er fiber using spatially and spectrally resolved imaging," presented at the Lasers and Electro-Optics and Conference on Quantum Electronics and Laser Science Conf., Paper No., CWD4 (2009).
9. J. W. Nicholson, J. Fini, J. Jasapara, A. DeSantolo, E. Monberg, and F. Dimarcello, "Measuring the modes of optical fibers using S2 imaging," presented at the *Lasers and Electro-Optics and Quantum Electronics and Laser Science Conf.* (2010).
10. J. Bromage, C. Dorrer, M. J. Shoup III, and J. D. Zuegel, "Optimizing injection into large-mode-area photonic crystal-fiber amplifiers by spatially resolved spectral interferometry," presented at the Lasers and Electro-Optics and Conference on Quantum Electronics and Laser Science Conf., Paper No. CWD3 (2009).
11. B. G. Ward, D. M. Wright, C. J. Eicholtz, and C. G. Carlson, "Photonic crystal fiber with resonant-coupling higher-order-mode suppression," *Proc. SPIE*, **7580**, 758011-1-9 (2010).
12. B. G. Ward, "Bend performance-enhanced photonic crystal fiber with anisotropic numerical aperture," *Opt. Express* **16**, 8532–8548 (2008).
13. J. C. Jasapara, M. J. Andrejco, A. D. Santolo, A. D. Yablon, Z. Várallyay, J. W. Nicholson, J. M. Fini, D. J. DiGiovanni, C. Headley, E. Monberg, and F. V. DiMarcello, "Diffraction-limited fundamental mode operation of core-pumped very-large-mode-area Er fiber amplifiers," *IEEE Sel. Top. Quantum Electron.* **15**, 3–11 (2009).

Biographies and photographs of the authors not available.